



**PHILIPS**

IQon Spectral CT

# True Spectral Imaging

Now, with the IQon Spectral CT,  
every scan can be spectral on demand.  
There's always a way to make life better.

innovation  you



# Therapeutic Proton Beam Range Measurement with EBT3 Film and Comparison with Tool for Particle Simulation

Nuri Lee<sup>1</sup>, Chankyu Kim<sup>2</sup>, Mi Hee Song<sup>1</sup>, Se Byeong Lee<sup>2</sup>

<sup>1</sup>Department of Radiation Oncology, National Medical Center, Seoul, <sup>2</sup>Proton Therapy Center, National Cancer Center, Goyang, Korea

**Received** 6 December 2019

**Revised** 18 December 2019

**Accepted** 18 December 2019

## Corresponding author

Nuri Lee

(nurilee@nmc.or.kr)

Tel: 82-2-2260-7331

Fax: 82-504-099-2746

**Purpose:** The advantages of ocular proton therapy are that it spares the optic nerve and delivers the minimal dose to normal surrounding tissues. In this study, it developed a solid eye phantom that enabled us to perform quality assurance (QA) to verify the dose and beam range for passive single scattering proton therapy using a single phantom. For this purpose, a new solid eye phantom with a polymethyl-methacrylate (PMMA) wedge was developed using film dosimetry and an ionization chamber.

**Methods:** The typical beam shape used for eye treatment is approximately 3 cm in diameter and the beam range is below 5 cm. Since proton therapy has a problem with beam range uncertainty due to differences in the stopping power of normal tissue, bone, air, etc, the beam range should be confirmed before treatment. A film can be placed on the slope of the phantom to evaluate the Spread-out Bragg Peak based on the water equivalent thickness value of PMMA on the film. In addition, an ionization chamber (Pin-point, PTW 31014) can be inserted into a hole in the phantom to measure the absolute dose.

**Results:** The eye phantom was used for independent patient-specific QA. The differences in the output and beam range between the measurement and the planned treatment were less than 1.5% and 0.1 cm, respectively.

**Conclusions:** An eye phantom was developed and the performance was successfully validated. The phantom can be employed to verify the output and beam range for ocular proton therapy.

**Keywords:** Proton therapy, Melanoma, Radiotherapy setup errors, Radiotherapy computer-assisted, Film dosimetry

## Introduction

Proton therapy is significantly effective for treating ocular tumors because of the Bragg peak feature. The most common primary intraocular tumor is choroidal melanoma. Tumors arising in the choroid have a 30% chance of metastasis at 5 years, whereas iris and conjunctival melanomas have a considerably lower risk. Tumor size is the most important prognostic factor. The proton radiotherapy of

ocular melanoma results in overall satisfactory local control rates of 97% at 5 years, 96% at 10 years, and 94% at 15 years, with overall tumor specific survival rates of 91% at 5 years, 83% at 10 years, and 79% at 15 years.<sup>1)</sup> Small melanomas are typically asymptomatic, and it can be difficult to differentiate them from various benign conditions. Small tumors can be enucleated with indium-125 or ruthenium-106 plaque brachytherapy, protons, or other local treatment options.<sup>2)</sup>

Eye treatment using proton therapy should be evalu-

ated to determine the accuracy and quality of treatment, and ocular treatment validation is essential. Gradoudas et al.<sup>3)</sup> introduced proton therapy for patients with ocular melanoma in 1974. Subsequently, Goitein and Miller<sup>4)</sup> developed a computer-based treatment named EYEPLAN,<sup>5)</sup> which has been used to treat over 20,000 patients worldwide. Reducing the risk of side effects requires more accurate prediction of the dose to which critical organs and structures are exposed. To address this issue, Newhauser et al.<sup>6)</sup> proposed the use of Monte Carlo simulations with an analytical model for EYEPLAN measurements.

Radiochromic film dosimetry is suitable for radiotherapy applications, particularly particle therapy.<sup>7,8)</sup> Radiochromic EBT3 films consist of two 0.125-mm-thick layers of polyester foils and a 0.030-mm active layer sandwiched between the polyester layers, resulting in a total thickness of 0.280 mm.<sup>9)</sup> The films can perform dose characterization and verification and determine the quality of radiation beams. The technique provides several advantages. For example, other tools for the 2D measurements of dose distribution have limited resolution. However, films can provide extremely high resolution for optical density changes, which stabilize rapidly within 2 hours, even though the recommended duration for measurement is 8 hours. Additionally, dose to response uniformity is good at less than 1.5%.<sup>10)</sup> Finally, specific information such as reference values or an electrometer within ion chambers are not required.

However, EBT3 films have disadvantages such as energy dependence and the requirement for a chemical response.<sup>11)</sup> Radiochromic EBT3 films show the same dosimetry response to proton beams as their counterparts for protons in the proximity of the Bragg peak, specifically with regard to underestimating the dose in the peak region.<sup>10)</sup> This behavior must be understood to analyze the quenching of the proton beam at the Bragg peak. The quenching effect is directly related to the linear energy transfer (LET) of radiation particles (Birks 1964<sup>12)</sup>, Torrisi 2000<sup>13)</sup>). Information about the LET distribution in a phantom is necessary to account for this effect.<sup>14)</sup>

The aim of this study was to create a method for the simple and accurate measurement of the proton depth profile. Accurate measurement requires a correction factor for the quenching effect, which depends on the energy used for

ocular treatment. In this study, proton beam therapy was used for eye tumor treatment with low energy (approximately 60 MeV). Range checking was improved using EBT3 films, and predicted dose was analyzed using output values with ionization chamber. The tool for particle simulation (TOPAS) was used for performing accurate simulation with the Monte Carlo wrap program.

## Materials and Methods

### 1. Patient delivery quality assurance

The monitor units (MUs) used for proton therapy treatment are required during patient quality assurance (QA). Generally, patient delivery QA requires a water phantom, ion chambers, and a diode-type reference chamber. The resolution of the diode (SFD Stereotactic; IBA, Schwarzenbruck, Germany) should be less than 2 mm, and farmer-type chamber rolls should be used as reference ion chambers. In addition, reference chamber checks must be performed for the calibration of the output for calculating patients' dose. In the diode-type chamber, the effective point for measurement which needs to obtain accurate value is less than 0.9 mm, the diameter of the active area is 0.6 mm, and the thickness of the active volume is 0.06 mm. Additionally, the film range is measured after proton irradiation. The depth profile can be measured to determine the proton beam range and spread-out Bragg peak (SOBP). This process identifies the matching parameters between planning using a treatment planning system and a convenient algorithm from IBA (CONVALGO). This CONVALGO is a sort of simulation data which IBA supports. Eye treatment is performed after patient QA, and the MU utilized for patient treatment with an ionization chamber at the middle of the SOBP is verified.

### 2. New designed phantom

A phantom was designed considering the water equivalent value for PMMA, i.e., 1.16. The depth profile of the proton beam cannot be measured using the EBT3 film because of the quenching effect of film; therefore, an entry's slope is required for irradiation. In addition, the slope of the phan-



tom provides an angle that does not require the correction of the proton beam depth measured in water. In this case, the new specifications for the phantom are as follows: a height of 6 cm, a width of 10.21 cm, and a length of 11.84 cm (Fig. 1). This is because the range of the proton beam for ocular patients is less than 10 cm. A smaller phantom provides an accurate proton beam range and save time for the process of setup.

The PMMA phantom can be used for two types of measurements: in vivo dosimetry with film QA and absolute dose measurement with a pinpoint chamber (PTW 31014). The new eye treatment phantom is separated into two parts. One part is used for measuring the range for placing an EBT3 film on PMMA, while the other part consists of a

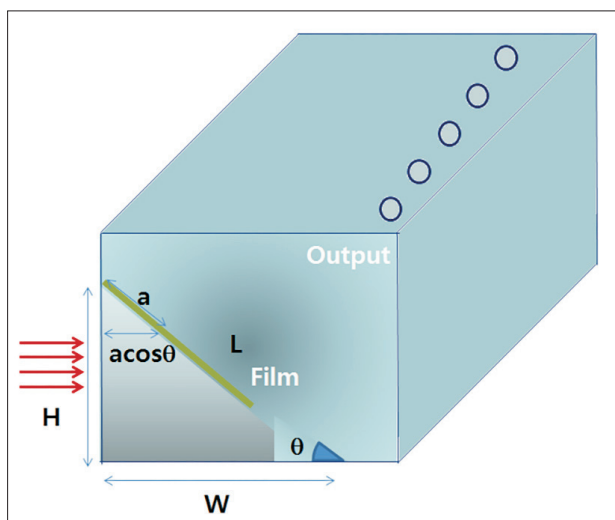


**Fig. 1.** The scheme of fabricated polymethyl-methacrylate (PMMA) new phantom.  $a$ , a certain variable;  $L$ , length of PMMA phantom's slope;  $H$ , height of PMMA phantom;  $W$ , width of PMMA phantom.

chamber hole inside which PMMA is placed. The two parts of the phantom are necessary because one measures the proton beam depth and energy and the other determines the dose for patient treatment.

### 3. Radiochromic film measurement

Gafchromic EBT3 films were used to measure the proton beam depth. Calibration curves were created for an incident proton energy of 113.9 MeV (range at water depth is  $10 \text{ g/cm}^2$ ) in the proximal region at a beam entry's area; approximately 2 to  $3 \text{ g/cm}^2$ ; the closer to the bragg peak has been reaching the quenching effect. The films used to construct the calibration curve were obtained from the same batch as that used for measurements and stabilized for 8 hours between irradiation and scanning.<sup>9)</sup> The irradiated films were scanned in a consistent orientation using Epson 10000XL and 11000XL (Epson, Long Beach, CA, USA) at a resolution of 75 dpi (0.3387 mm). The dose-response curve equation was obtained using 5th degree interpolation data, which were generated for doses ranging from 0 to 10 Gy in the red channel.

### 4. Setup for phantom

The fixed gantry for proton therapy with an eye snout consisted of a beam field with a diameter of 6 cm, which was set up as a circular area with a diameter of 4 cm. This proton beam was used in the single scatter mode without an initial scatter at the location of phantom to open a brass block and installed at the end of the eye snout. The distance between the ends of the eye snout and the center

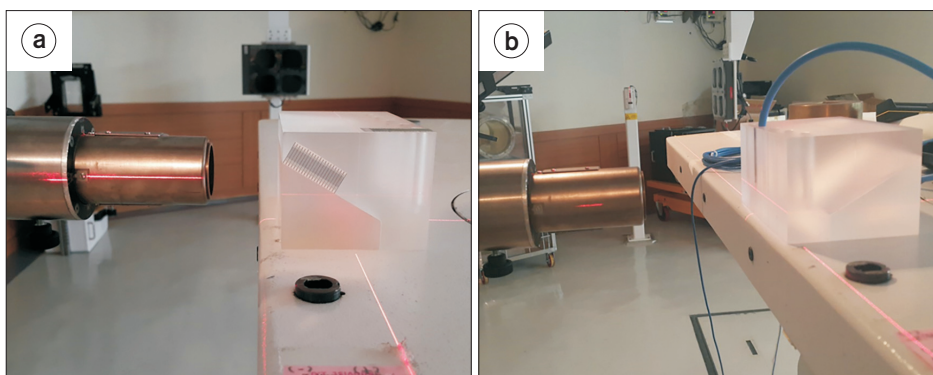


**Fig. 2.** The setup of fabricated new phantom for ocular treatment within 2nd check; depth and dose. (a) Measurement of range with EBT3 film, (b) confirmation of dose using ionization chamber.

of the PMMA phantom was 20 cm (Fig. 2). Fig. 2 shows the schematic of the side view of the setup utilized to measure the beam range and dose for patients. There was an air gap between the ends of the water phantom on the beam path. The size of the eye beam field at the end of the beam pipe was approximately 2.5 cm. The proton beam field size was increased owing to interactions with the materials in the beam delivery system, such as the ion chambers, single scatter, and range modulator. When the 2.5-cm-diameter core of the eye treatment beam was injected from the nozzle beam pipe into the beam delivery system in the fixed-gantry room, the proton beam was spread out owing to scattering by the materials in the beam path. The proton beam range was defined as the depth from the water

surface to 90% of the peak position proximal to 90% of the peak position in the distal falloff.

## 5. TOPAS

TOPAS wraps and extends the Geant4 simulation toolkit to provide an easy-to-use application for medical physicists. TOPAS serves as a parameter control system while Geant4 is a framework for simulating the fundamental physical process for the passage of particles through matter. The aim of TOPAS is to make proton simulation reliable and repeatable. It can improve accuracy and reduce the error caused by the setup. Additionally, TOPAS is an open access tool, and it can be easily used by beginners.<sup>15)</sup>

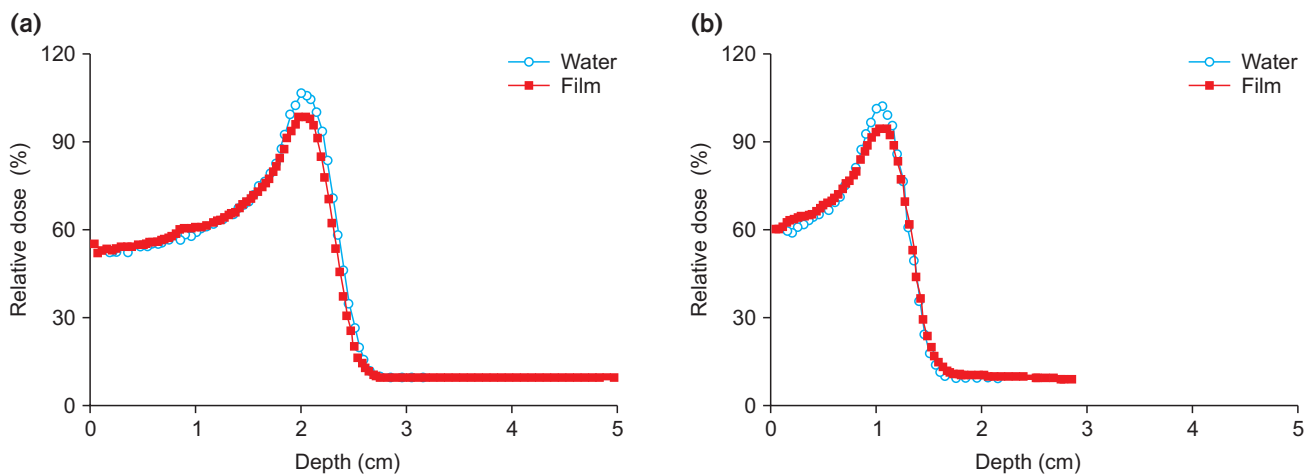


**Fig. 3.** The energy dependence results of depth dose profiles at Bragg peaks. (a) Bragg peak of 46.0 MeV, (b) Bragg peak of 32.0 MeV.

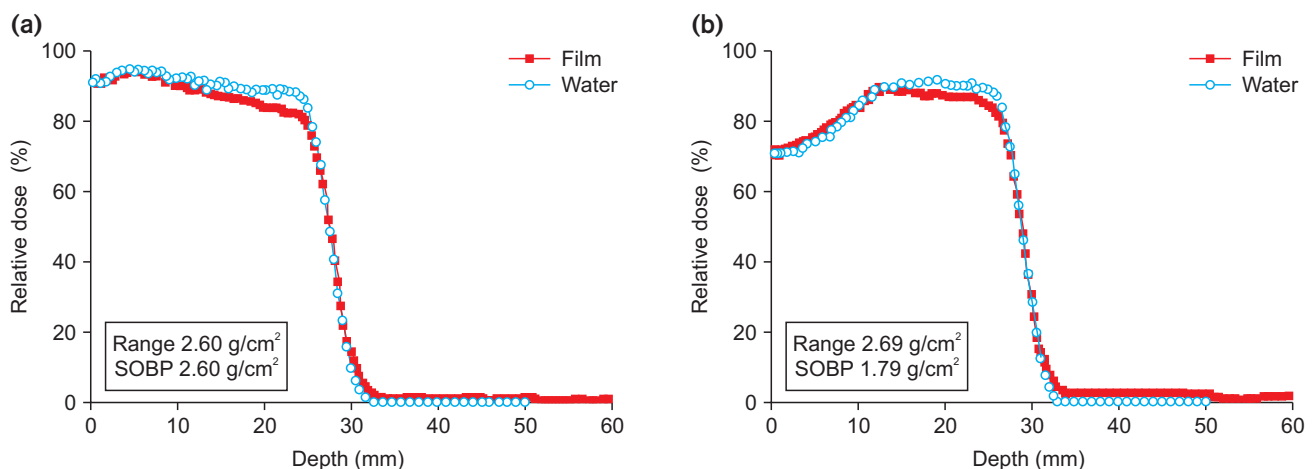


**Fig. 4.** The Comparison depth dose profiles between EBT3 film and water. (a) Represents the same value of beam range and SOBP, full modulation case, (b) general case of proton therapy for ocular tumors. SOBP, spread-out Bragg peak.

## Results

The beam conditions of the patient's proton treatment plan were delivered to the EBT3 film on the new QA phantom. A dose of 200 cGy was delivered to the films at the point depth of the Bragg peak. Fig. 3 shows the depth-dose curves for the two measured proton beams. The curves were compared to the dose-depth profile for the Bragg peak between water-based measurements and the EBT3 films. The red line represents film data while the blue line

represents the water phantom at the same energy: 46.0 MeV (Fig.3a) and 32.0 MeV (Fig.3b). The results exhibit good agreement with the profile at the proximal position of the beam range. The depth profile and energy have a linear relationship in this low energy region. The quenching effect on the EBT3 films is observed around the peak position. The quenching effect is more apparent when energy is high, and it is less than 10% at the top of the Bragg peak at low energy. Previous studies have shown the 10% quenching effect is observed at an energy of over 100 MeV. How-

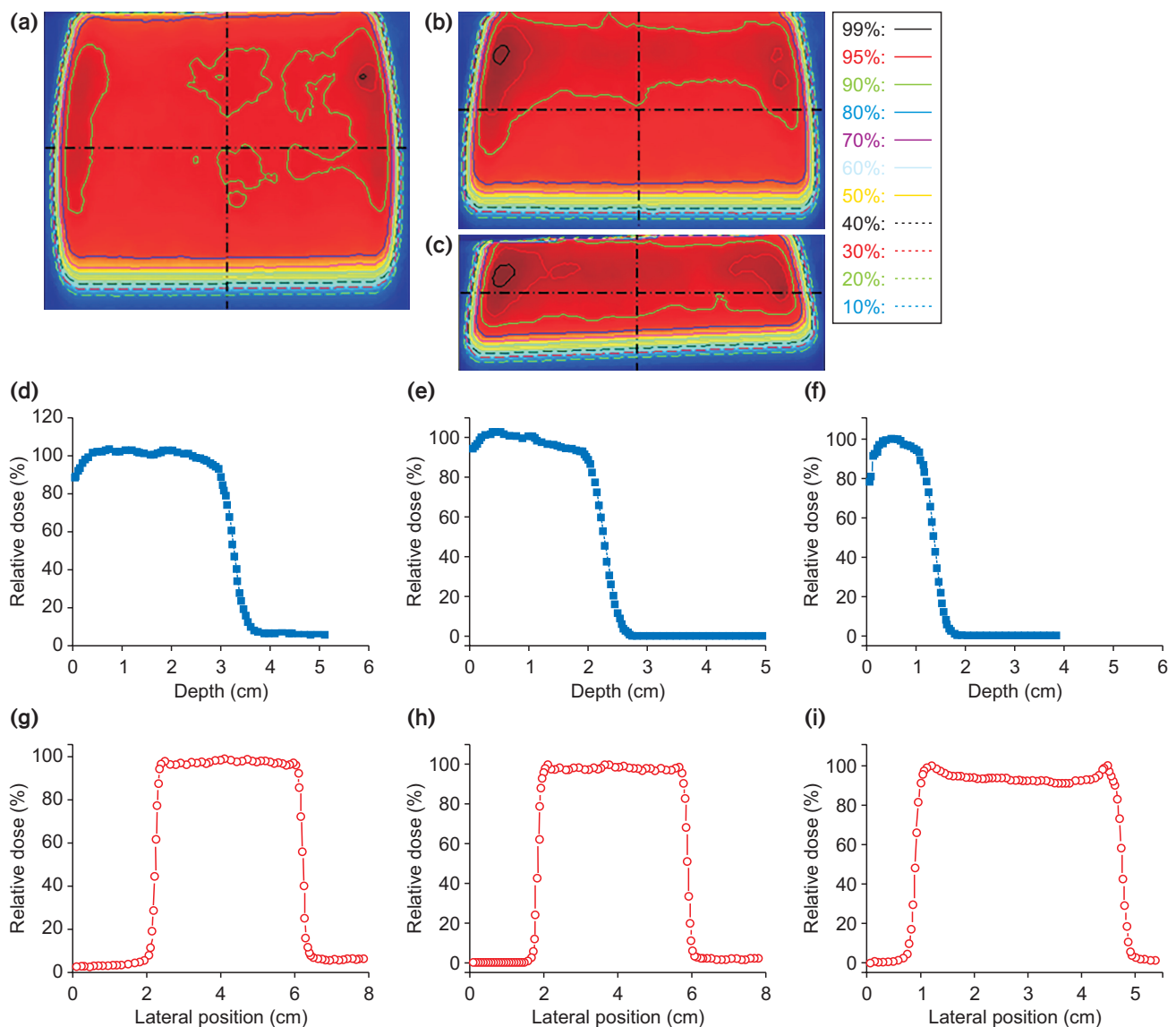


**Fig. 5.** The EBT3 film analysis ocular tumor data which depend on proton energy. EBT3 film data (a) 57.7 MeV, (b) 46.0 MeV, and (c) 32.0 MeV. Depth dose profiles (d) 57.7 MeV, (e) 46.0 MeV, and (f) 32.0 MeV, and lateral profilers from EBT3 film (g) 57.7 MeV, (h) 46.0 MeV, and (i) 32.0 MeV.

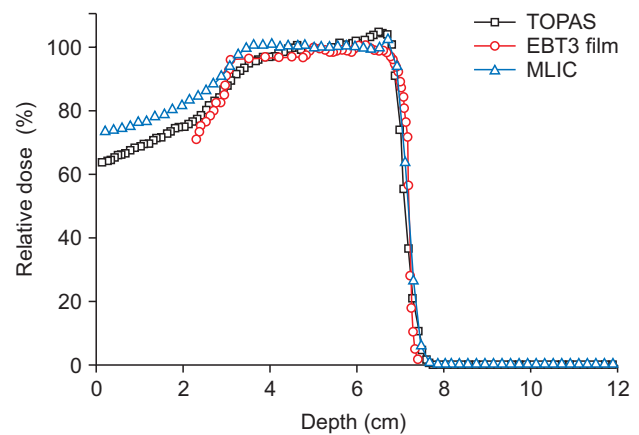
ever, energy is less than 100 MeV in this work.<sup>16)</sup> Therefore, the depth-dose profile for the EBT3 films may not require other correction factors for the measurement of the beam range.

Fig. 4 shows the comparison of the range and SOBP measurement using the water phantom and film dosimetry for the new QA phantom. The beam was formed for each patient using the scatter and range modulator, resulting in a flat depth-dose distribution. The final lateral shape of the proton beam was formed by a brass collimator, which was individually prepared for each patient according to tumor shape and position. The proton beam depth profiles observed with the water phantom and films were different. Fig. 4a presents the general case for a full modulation proton beam, and Fig. 4b presents the case for the same beam range and SOBP. Both images are in good agreement with the percent depth-dose profiles. The profile data matched the beam range at the entrance dose between measurements with the phantom and in the water. This is because the proximal region is not affected by the quenching effect and the beam range corresponds with the distal falloff region.

The RIT 113 film dosimetry system software (V.5.2.; RIT Inc., Denver, CO, USA) was used to measure the range, symmetry, and flatness of the beam, as shown in Fig. 5. Irradiated and exposed films were scanned, and lateral profiles were extracted from perpendicular and parallel films. The beam range used for eye tumors was small, with a diameter of approximately 2.5 to 3 cm. The final lateral shape of the proton beam was formed by a brass collimator, which was individually prepared for each patient according to tumor shape and position. The lateral profile of the proton beam was measured with the EBT3 film in the

fully modulated SOBP.

Fig. 5 shows the analysis results for the EBT3 films for an ocular patient plan. The RIT 113 software was employed for film evaluation during dose field mapping. Fig. 5a-c show the dose distribution according to the dose, Fig. 5d-f show the depth-dose profile obtained using the EBT3 films, and Fig. 5g-i show the lateral profile of the proton beam. The symmetry, flatness, and quality of the beam were determined using the RIT 113 software (Table 1). The lateral profiles were measured from the films irradiated parallel to the beam axis.<sup>17)</sup> The main characteristics of the lateral distribution are shown in Table 1. The clinical tolerances adopted for the treatments were symmetrical around 3%, and the penumbra was less than 1.5 mm.



**Fig. 6.** The depth dose profiles with TOPAS, EBT3 film and MLIC. TOPAS, tool for particle simulation; MLIC, multilayer ionization chamber.

**Table 1.** The properties of different proton beam energies with EBT3 films

Variable	Proton beam energy (MeV)		
	57.7	46.0	32.0
Range (g/cm <sup>2</sup> )	3.08	2.04	1.06
SOBP (g/cm <sup>2</sup> )	2.95	2.04	1.06
Symmetry (%)	1.98	3.39	3.77
Flatness (%)	2.40	3.08	3.40
Penumbra (mm)	1.41	1.41	1.41

SOBP, spread-out Bragg peak.

**Table 2.** Comparison of depth and dose data obtained from single passive mode proton therapy performed using water and fabricated phantoms

Range with water phantom (cm)	Range with EBT3 film (cm)	Differences of range (cm)	Error (%)
2.64	2.57	0.07	1.27
3.16	3.07	0.09	-0.30
1.06	1.16	-0.10	-1.52
2.06	2.08	-0.02	-1.46
2.60	2.48	0.12	-1.23
2.70	2.57	0.13	-0.70
2.61	2.62	-0.01	-0.07
2.2	2.17	0.03	1.40
1.8	1.78	0.02	-0.76
1.62	1.58	0.04	0.0

## Discussion

Ocular proton therapy requires high accuracy and resolution; therefore, quality control using a 3D water phantom is recommended for every treatment. However, there is no second check of patient delivery data or a simple process for quality control. To solve this problem, a simple phantom was developed in this study for measurements using TOPAS. Fig. 6 shows the depth-dose profile results obtained from TOPAS, the EBT3 films, and the multilayer ion chamber. The new phantom can measure the beam depth profile and current value for patient dose. Table 2 shows the beam depth profiles obtained using the water phantom and new PMMA phantom. The data for the depth range and output factor for ocular therapy are provided for 10 patients. The differences of proton beam measurement from most patients' plans between water and EBT3 film were smaller than 1.2 mm and less than 4% of the treatment range. In addition, the output for which calculated patients' dose were less than 1.5%. These data were quite sensitive since this case had the shortest range with a modulated beam.

## Conclusions

The preliminary results show the depth-dose profiles obtained using the EBT3 films. The proton therapy has originally uncertainty, but the lower energy has less quenching effect on the EBT3 films promising candidate for dosimetry in various applications.<sup>11)</sup> High energy causes quenching at the EBT3 films. However, the proposed method uses relatively low energy below 60 MeV for ocular tumors. We obtained the beam range from the EBT3 films using an extremely simple and useful technique to check the proton beam range. Proton therapy for eye treatment provides the advantages of precise target conformity and a low integral dose with negligible secondary neutron doses.<sup>18)</sup> A new eye phantom was developed, and its performance was evaluated successfully. The phantom was useful for verifying the output and beam range for ocular proton therapy.

## Acknowledgements

This work was supported by Policy Research Program funded by National Medical Center, Research Institute (grant number: NMC2018-MS-04).

## Conflicts of Interest

The authors have nothing to disclose.

## Availability of Data and Materials

All relevant data are within the paper and its Supporting Information files.

## References

1. Piersimoni P, Rimoldi A, Riccardi C, Pirola M, Molinelli S, Ciocca M. Optimization of a general-purpose, actively scanned proton beamline for ocular treatments: Geant4 simulations. *J Appl Clin Med Phys*. 2015;16:261-278.
2. Barrett A, Dobbs J. Practical radiotherapy planning. 4th ed. London: Hodder Arnold; 2009.
3. Gradoudas ES, Goitein M, Koehler A, Constable IJ, Wagner MS, Verhey L, et al. Proton irradiation of choroidal melanomas. Preliminary results. *Arch Ophthalmol*. 1978;96:1583-1591.
4. Goitein M, Miller T. Planning proton therapy of the eye. *Med Phys*. 1983;10:275-283.
5. Koch N, Newhauser W. Virtual commissioning of a treatment planning system for proton therapy of ocular cancers. *Radiat Prot Dosimetry*. 2005;115:159-163.
6. Newhauser W, Koch N, Hummel S, Ziegler M, Titt U. Monte Carlo simulations of a nozzle for the treatment of ocular tumours with high-energy proton beams. *Phys Med Biol*. 2005;50:5229-5249.
7. Vadrucci M, Esposito G, Ronsivalle C, Cherubini R, Maracino F, Montereali RM, et al. Calibration of GafChromic EBT3 for absorbed dose measurements in 5 MeV proton beam and (60)Co  $\gamma$ -rays. *Med Phys*. 2015;42:4678-4684.
8. Pai S, Das IJ, Dempsey JF, Lam KL, Losasso TJ, Olch AJ, et al. TG-69: radiographic film for megavoltage beam dosimetry. *Med Phys*. 2007;34:2228-2258.



9. Sipilä P, Ojala J, Kaijaluoto S, Jokelainen I, Kosunen A. Gafchromic EBT3 film dosimetry in electron beams - energy dependence and improved film read-out. *J Appl Clin Med Phys.* 2016;17:360-373.
10. Reinhardt S, Hillbrand M, Wilkens JJ, Assmann W. Comparison of Gafchromic EBT2 and EBT3 films for clinical photon and proton beams. *Med Phys.* 2012;39:5257-5262.
11. Sorriaux J, Kacperek A, Rossomme S, Lee JA, Bertrand D, Vynckier S, et al. Evaluation of Gafchromic® EBT3 films characteristics in therapy photon, electron and proton beams. *Phys Med.* 2013;29:599-606.
12. Birks JB. *Theory and Practice of Scintillation Counting.* New York: Pergamon; 1964.
13. Torrisi L. Plastic scintillator investigations for relative dosimetry in proton-therapy. *Nucl Instrum Methods Phys Res, Sec B.* 2000;170:523-530.
14. Wang LL, Perles LA, Archambault L, Sahoo N, Mirkovic D, Beddar S. Determination of the quenching correction factors for plastic scintillation detectors in therapeutic high-energy proton beams. *Phys Med Biol.* 2012;57:7767-81. doi: 10.1088/0031-9155/57/23/7767.
15. Chung K, Kim J, Kim DH, Ahn S, Han Y. The proton therapy nozzles at Samsung Medical Center: a Monte Carlo simulation study using TOPAS. *J Korean Phys Soc.* 2015;67: 170-174.
16. Zhao L, Das IJ. Gafchromic EBT film dosimetry in proton beams. *Phys Med Biol.* 2010;55:N291-N301.
17. Vatnitsky SM. Radiochromic film dosimetry for clinical proton beams. *Appl Radiat Isot.* 1997;48:643-651.
18. Kim DW, Chung WK, Shin J, Lim YK, Shin D, Lee SB, et al. Secondary neutron dose measurement for proton eye treatment using an eye snout with a borated neutron absorber. *Radiat Oncol.* 2013;8:182.